IEEE Access
Multidisciplinary | Rapid Review | Open Access Journal

Received May 29, 2019, accepted June 10, 2019, date of publication June 13, 2019, date of current version July 1, 2019.

Digital Object Identifier 10.1109/ACCESS.2019.2922644

Recent Progress on Probe-Based Storage Devices

ZHI-GAO LIU AND LEI WANG

School of Information Engineering, Nanchang Hangkong University, Nanchang 330063, China

Corresponding author: Lei Wang (leiwang@nchu.edu.cn)

This work was supported in part by the U.S. Department of Commerce under Grant BS123456.

ABSTRACT Prosperity of information technology triggers a tremendous amount of digital data that needs to be stored by storage memories with ultra-high capacity. Although probe-based memory has exhibited its superb storage merits, its developments to date, however, remain slow due to several physical limits. In order to overcome its drawbacks, and to further advance probe storage technologies, a comprehensive review regarding the current status and future prospect of probe-based memories become of importance. In this paper, we first presented the physical principles of various reported probe-based memories and their respective advantages/disadvantages, as well as their current status. Subsequently, up-to-date progress made on these probe memories and some novel probe memories concepts is proposed. The prospect of a probe-based memory device is finally predicted.

INDEX TERMS Phase-change materials, probe, capping, transmission.

I. INTRODUCTION

Today digitalization has been found on majority of industries that include education, military, entertainment, and finance. This obviously generates vast amount of digital data which becomes ubiquitous in every citizen's daily life. The total amount of global data was reportedly predicted to achieve 33 Zettabytes (ZB) and 175 Zettabytes in the year of 2018 and 2025, respectively [1]. To outperform the storage demand stemming from all this data creation, the storage capacity of conventional mass storage devices such as magnetic hard disk drives (HDDs), magnetic tape, and optical disc drives (ODDs), needs to be sharply augmented. However, their respective physical drawbacks (e.g., superparamagnetic limits for HDDs and magnetic tape, and diffraction limits for ODDs) severely limits the storage potential of conventional storage devices, and make their storage capacity far behind the current storage demand [2]–[7], as reflected in Figure 1. Under this circumstance, it is urgent to explore some emerging mass storage devices that exhibit much higher storage capacity to meet storage requirements from both consumers and industries.

Probe-based storage memory used to be one of the most promising candidates for next-generation mass storage device. Probe memory makes use of a nanoscale probe that is originally used by scanning probe microscopy (SPM) to map surface topography [8], to change the physical properties of the storage media. Such a process is usually named as 'Recording'. The region of storage media with resulting different properties can be discriminated from rest part of storage media through external stimulus, which is called 'Readout'. Such mechanisms are schematically in Figure 2.

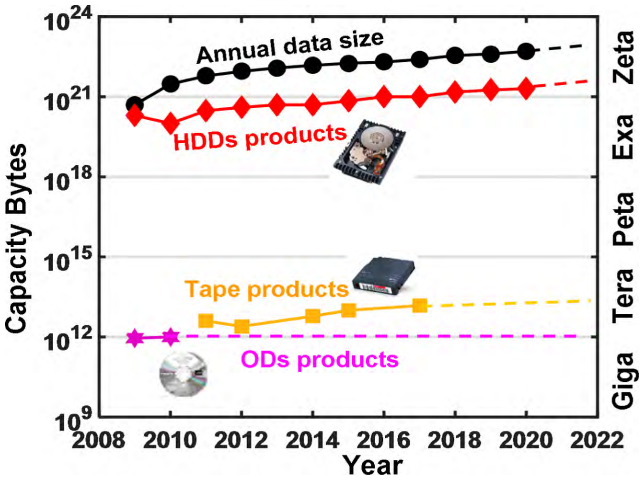

FIGURE 1. Storage capacity roadmap of conventional mass storage devices.

As applied stimulus is injected to the storage media via a SPM probe, the size of the recorded region strongly depends on the apex diameter of the probe, meaning that using a nanoscale probe with ultra-small apex may enable an ultra-small recorded region and consequently lead to ultra-small storage capacity. Triggered by this hypothesis, several types of probe-based storage memories, including

The associate editor coordinating the review of this manuscript and approving it for publication was Cristian Zambelli.

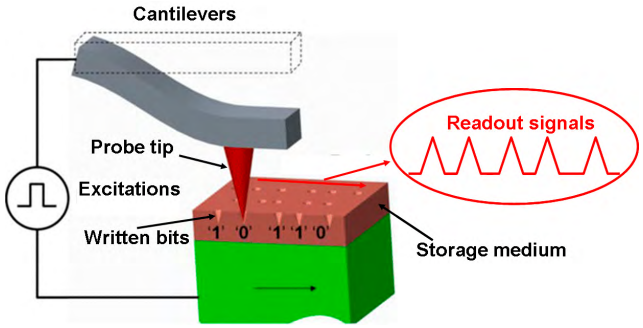

FIGURE 2. Recording and readout mechanism of probe-based memories.

thermo-mechanical probe memory [9]–[14], magnetic probe memory [15]–[20], ferroelectric probe memory [21]–[26], phase-change electrical probe memory [27]–[34], and phase-change thermal probe memory [35], have been sequentially proposed, and their potential of having high storage capacity have also been demonstrated either by experiments or by simulations. Nevertheless, the study on probe-based memory still remains in laboratory level during last decade and its commercialization is yet to be realized due to some insurmountable limits such as probe wear and energy consumption. To revive public attention to probe-based memory, significant improvements on aforementioned probe memories, as well as the debut of some innovative probe storage means, are intensely required. It is therefore instructive to have a comprehensive review concerning the physical principles, history, state-of-the-art, and prospect of probe-based memory to regain researchers' interest in this potential, but not fully explored field.

In this review, we first presented the physical principles of various reported probe-based memories and their respective advantages/disadvantages, as well as their current status. Subsequently, up-to-date progress made on these probe memories and some novel probe memories concepts are proposed. The prospect of probe-based memory device is finally predicted.

II. CONVENTIONAL PROBE-BASED MEMORIES

Probe memory families, as illustrated in Figure 3, comprise thermo-mechanical probe memory, magnetic probe memory, ferroelectric memory, phase-change electrical probe memory, and phase-change thermo probe memory. The key components of thermo-mechanical probe memory, also known as 'Millipede' memory, are polymer storage medium and a localized heating element. As can be seen from Figure 3(a), the probe tip with a localized heating element, usually made of low-doped resistive silicon, integrated at its base, is heated to glass transition temperature (∼400 °C), and is subsequently pushed into the polymer medium. The resulting high temperature enables melting of polymer medium and readily makes probe tip penetrate through the media to create an indentation with similar size to probe tip. Therefore, the regions with and without indentations can be used to represent binary bits '1' and '0', respectively. To erase the previously written bit, probe tip is pulled back from the indentation that is thus flatten by the consequent surface tension [9]. The readout process is performed by integrating a read resistor whose resistance is sensitive to temperature at the cantilever. Penetrating probe tip through the indentation reduces the distance between tip and substrate acting as a heat sink, and significantly lowers the temperature inside the read resistor. Such a temperature change can be considered as a readout signal.

The storage capacity of thermo-mechanical probe memory can be remarkably enhanced by choosing proper probe tip and storage medium. It was reported that the rim size of the indentation determines the bit pitch, and thus becomes a critical factor for the resulting areal density [12]. Therefore, a probe with smaller tip apex and a shorter indentation depth are usually preferable to compact the rim size, thereby allowing for higher recording density. The storage medium of thermo-mechanical probe memory usually include Dies-Adler (DA) polymer [11] and polyaryletherketone (PAEK) polymer [12] due to their advantageous storage features such as high wear resistance, easy deformation, and great thermal stability. The possibility of using DA and PAEK polymers to achieve 1 Terabits/inch^2 (Tbit/in^2) and 4 Tbit/in^2 have been demonstrated, respectively [11]–[12], as demonstrated in Figure 4(a). Shape memory alloy (SMA) is an alternative storage medium for thermo-mechanical probe storage due to its less susceptibility to environmental noise, high thermal conductivity, and low operating temperature [36]. These encouraging traits can effectively reduce the energy consumption during write process and result in a faster erasing operation. However, as thermo-mechanical probe memory makes use of thousands of probe tips to record data simultaneously, tip and sample wear is hence considered as a formidable issue, severely impairing the resulting density. Another issue of thermo-mechanical probe memory arises from the fact that a heated probe tip is always required for write, erasing and readout processes, which costs extra energy consumption.

The recording process of magnetic probe memory, as illustrated in Figure 3(b), is realized by reversing the magnetization of a magnetic storage media via magnetic field emanated from the probe tip of magnetic force microscope (MFM). The MFM probe is subsequently brought in proximity to the previously written bit and the resulting magnetic force between the tip apex and magnetic bit actually deflects the cantilever up and down. Such position variation can be implemented as readout signals. As revealed by well-known Neel-Arrhenius law, reducing bit volume for higher recording density usually accompanies with the increase of crystalline anisotropy to maintain thermal stability. However, large crystalline anisotropy usually requires a strong magnetic field to reverse it, which can not be provided by MFM probe. This obviously limits the storage capacity of magnetic probe memory below 200 Gigabits/inch^2 (Gbit/in^2) [37]. One possible approach to strengthen the reverse magnetic field is to add an external field emanated from a small coil placed underneath the substrate to the original written field from

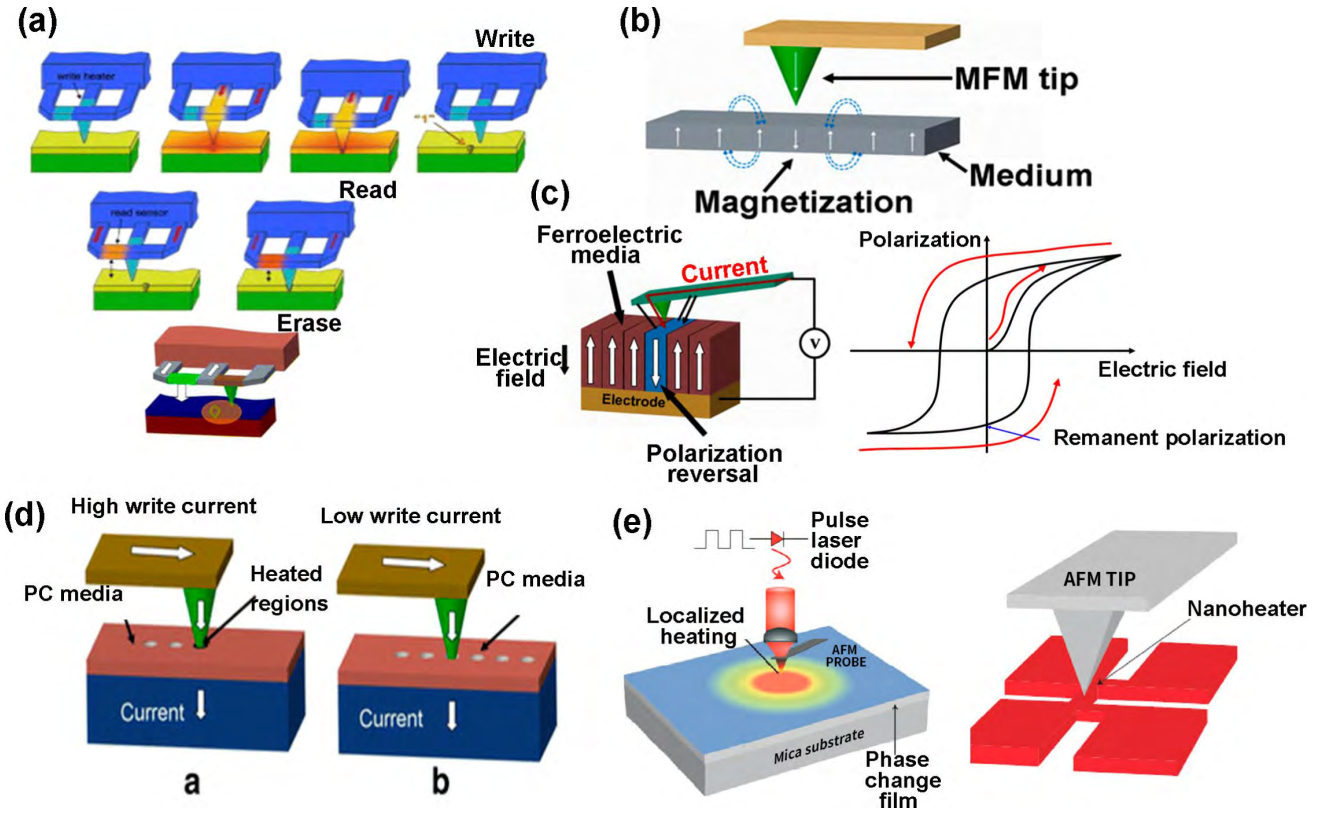

FIGURE 3. Physical principles of the conventional probe-based storage memories. (a) Write, read, and erase mechanism of thermo-mechanical probe memory; (b) write mechanism of magnetic probe memory; (c) write mechanism of ferroelectric probe memory (left) and its magnetic hysteresis (right); (d) phase-change electrical probe memory when operated in write mode (left) and readout mode (right); (e) write mechanism of phase-change thermal probe memory (left) and its experimental setup for measuring the temperature distribution of the nanoheater. (a) Reproduced with permission from [9]. (b)-(d) Reproduced with permissions from [14]. (e) Reproduced with permission from [35].

MFM probe [20], resulting in Figure 4(b). The feasibility of superimposing an external field to achieve 1.2 Tbit/in^2 has been verified [38]. Another scenario with immunity to the external magnetic field is to employ scanning tunneling microscope (STM) to locally heat the storage media through tunneling current to decrease the crystalline anisotropy [18]. It is therefore possible to reverse the magnetization of the heated region using a relatively low magnetic field, while maintaining a small bit volume. In addition to its write process, the readout of magnetic probe memory is also facing some physical barriers. A short tip-sample distance (< 10 nm) is generally required to allow for a readout image with high resolution. Nevertheless, MFM probe working within such a short distance usually causes a non-magnetic tip-sample interaction, thereby yielding unwanted topographic interference. A potential strategy to resolve this issue is to integrate a magneto-resistive sensor [39] or a magnetic field sensor for modern HDDs on the magnetic probe to highly improve the bit resolution [14].

The storage mechanism of ferroelectric probe memory stems from its spontaneous polarization that can be reversibly switched by applied electric field. In this case, binary codes '1' and '0' are represented by two different polarization states. The recording process of ferroelectric probe memory is accomplished by applying an electric field to a conductive probe to switch the polarization state of the ferroelectric storage medium, as shown in Figure 3(c). Differing from other probe memories, only '0' state can be detected by ferroelectric probe memory. As a result, '1' state needs to be erased back to '0' state prior to reading it, and the adopted erasing pulse (usually current pulse) is denoted as the readout signal for '1' state. Such a process is also named as 'destructive readout'. The fact that ferroelectric material presents much higher energy density than magnetic material implies that the undesired thermal fluctuation effect for ferroelectric material take places at much smaller volume than magnetic materials. For this reason, convention ferroelectric materials such as lead zirconate titanate (PZT) and $LiTaO_3$ have exhibited their capability of providing recording density up to 3.6 Tbit/in^2 [40] and 13 Tbit/in^2 [41], respectively, as revealed by Figure 4(c) Despite its density potential, the read/write cycles are largely increased due to such a 'destructive' readout mechanism, which may bring about severe fatigue.

Phase-change electrical probe memory, as described in Figure 3(d), depends on a reversible and rapid transition of Chalcogenide alloy between its crystalline state with long-range atomic order and amorphous state with short-range atomic order. During recording process, a current pulse is applied to the storage medium (Chalcogenide alloy in this

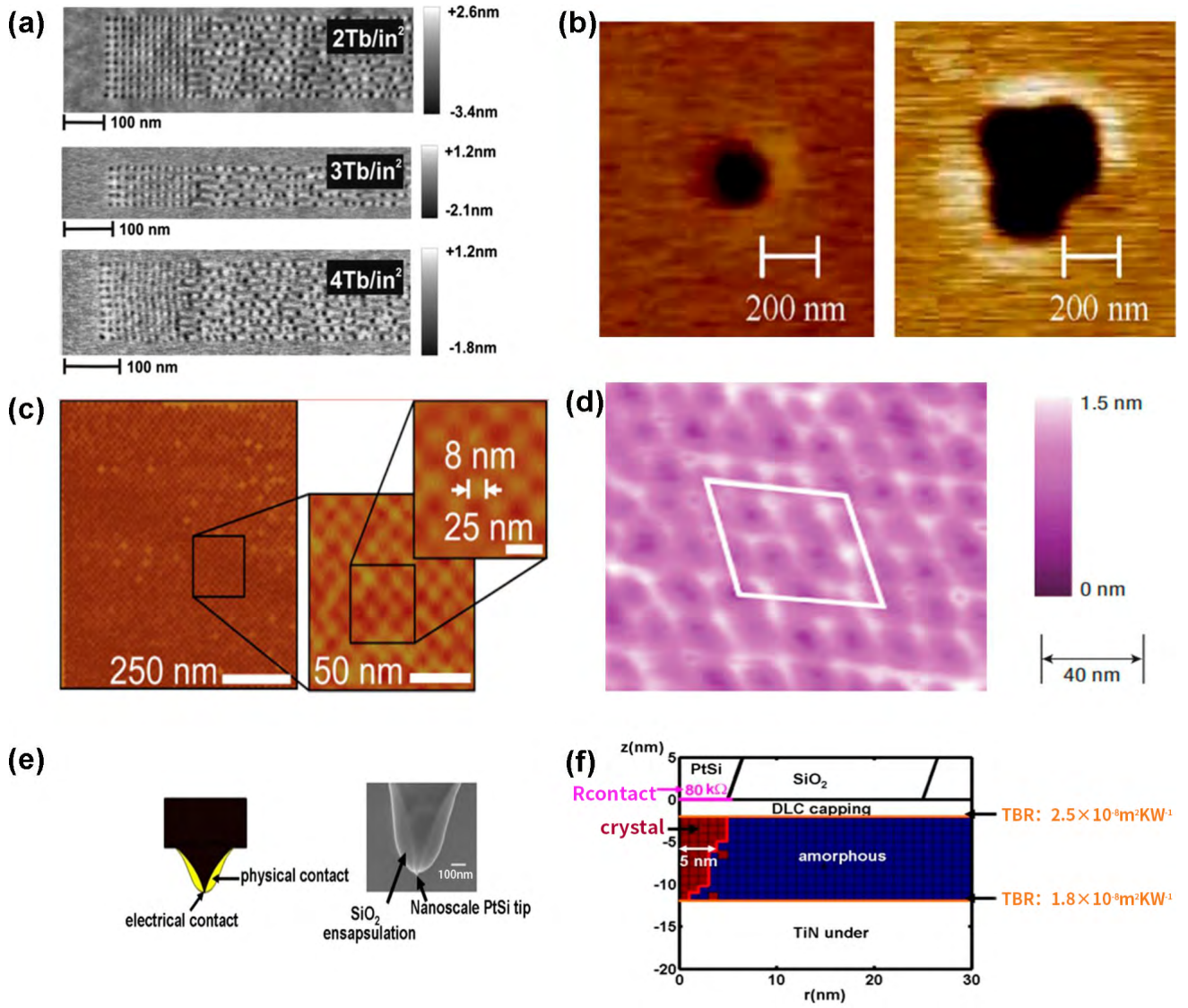

FIGURE 4. Achievable densities based on different probe storage memories (a) Random indentation patterns recorded by thermo-mechanical probe memory using PEAK polymer with normal spin coated sample (top), and ultraflat templated sample with different indent depth and partial erase ratio (center and bottom). (b) MFM images of written bits on magnetic sample with small applied field (left) and large applied field (right) from the coil. (c) 3.6 Tbit/in^2 ultrahigh storage density over a 1 × 1 μm^2 area using ferroelectric probe memory. (d)Topographic image of arrays of crystalline phase-change bits in an amorphous matrix at areal density of 3.6 Tbit/in^2. (e) Proposed and experimentally fabricated images of the encapsulated tip with ultra electrically conductive region at tip apex (left) and simulated crystalline bit based on an optimized media stack using electrical probe phase-change memory at areal density of 10 Tbit/in^2 (right). (a) Reprinted with permission from [12]. (b) Reprinted with permission from [20]. (c) Reprinted with permission from [40]. (d) Reprinted with permission from [35]. (e) Reprinted with permission from [34].

case) via a conductive probe, to heat the alloy either to the glass transition temperature to form crystallization, or to the melting temperature followed by a quick quench process to induce amorphization. The electrical resistivity difference between amorphous and crystalline states can be up to several orders of magnitude. Therefore, the readout process is performed by applying a voltage potential to the storage medium, and the resulting current variation can be treated as readout signals to differentiate the previously written bit from its background. Phase-change electrical probe memory has exhibited some storage merits that can not be reproduced by other probe memories. Unlike thermo-mechanical probe, the probe tip of phase-change electrical probe memory is not mandatory to be heated during recording process. This undoubtedly reduces the energy consumption per bit of phase-change electrical probe memory. Additionally, phase-change electrical probe memory inherits attractive storage features of Chalcogenide alloy originally used for phase-change random access memory, such as large data rate, long data retention, and great endurance [42]. Most importantly, as recorded/readout regions are mainly confined by the write/readout current, the tip apex of the electrical probe is only required to be electrically shape other than physically sharp. It is therefore possible to implement a probe tip with large physical diameter and small conductive diameter to provide high density while mitigating the tip wear.

Due to its aforementioned advantages, phase-change electrical probe memory has received considerable research efforts on both experimental design and performance simulation. Phase-change stack usually consists of a Chalcogenide alloy layer sandwiched between a capping layer and a under layer. The role of the capping layer is to protect the storage layer from wear and oxidation, whereas the under layer mainly serves as the bottom electrode to collect write/read currents. A theoretical model that consists of the Laplace equation, heat conduction equation, and JMAK equation, has been developed to mimic the corresponding electrical, thermal, and phase-transformation processes, respectively [28], [31]. According to this model, an optimized capping layer is made of diamond-like carbon (DLC) layer whose thickness, electrical conductivity and thermal conductivity vary between $2-10$ nm, $10-100\ \Omega^{-1}\mathrm{m}^{-1}$ and $0.5-5\ \mathrm{Wm}^{-1}\mathrm{K}^{-1}$, respectively. The under layer targeted to offer high write/readout current under a small excitation was optimized to be made of titanium nitride (TiN) layer with thickness, electrical conductivity and thermal conductivity ranging form 10 nm, $10^5\ \Omega^{-1}\mathrm{m}^{-1}$, and $3\ \mathrm{Wm}^{-1}\mathrm{K}^{-1}$, to 50 nm, $5\times10^5\ \Omega^{-1}\mathrm{m}^{-1}$, and $12\ \mathrm{Wm}^{-1}\mathrm{K}^{-1}$, respectively. The Chalcogenide layer is generally considered as the $Ge_2Sb_2Te_5$ alloy (also abbreviated as GST) that has been widely employed in PCRAM and conventional optical disc because of its fast switching speed, relatively low transition temperature, and superb stability at room temperature. The amorphous GST media was reported to exhibit an unique threshold switching characteristic that the resulting current suddenly undergoes a drastic increase once the applied voltage exceeds a so-called threshold voltage [43]. The threshold voltage can be simply described as a product of the threshold field and the GST layer thickness, meaning that a thin GST layer is highly desired in order to reduce the threshold voltage. In this case the GST layer thickness is optimized to vary between $5-10$ nm [31]. A silicon dioxide (SiO_2) encapsulated silicon (Si) probe with platinum silicide (PtSi) at tip apex has received intensive attention for phase-change probe memory. Doping PtSi at tip apex can not only enhance the electrical conduction capability due to the ultra-high electrical conductivity of PtSi, but also improve its anti-wear characteristic [44]. Coating such a probe with SiO_2 can effectively expand the contact area at tip-sample interface, whereby the interfacial pressure is reduced, consequently alleviating the tip wear [45], as described in Figure 4(e). The potential of using such an optimized architecture to achieve 10 Tbit/in^2 has been demonstrated [34]. The disadvantage of phase-change electrical probe memory mainly stems from its amorphization process that usually requires high temperature. Such a high temperature may accelerate the oxidation of DLC capping layer, and thermally harm the device. Additionally, erasing crystalline bits is generally accompanied with the re-crystallization of surround amorphous background, likely causing a readout error. For above reasons, the development of phase-change electrical probe memory has been decelerated during last decade.

Phase-change thermal probe memory consolidates the thermal probe previously used for thermal-mechanical probe memory with the Chalcogenide alloy used for phase-change electrical probe memory to realize its storage function, as indicated in Figure 3(e). During the recording process, a probe tip that is heated by a solid-state laser is brought in proximity to the Chalcogenide layer to induce the phase transformation through the dissipated heat energy. The readout process was conducted by detecting the impedance of a nanoheater that is in contact with the Chalcogenide layer. Owing to the thermal conductivity difference between crystalline and amorphous phases, the temperature of the nanoheater when in contact with phase-transformed region strongly differs from that when in contact with non-transformed region, thus regarded as readout signals. Phase-change thermal probe memory exhibits the capability of providing 3.3 Tbit/in^2 and over 100 write-read-erase cycles [35], as shown in Figure 4(d). However, such a readout mechanism drastically relies on lithographic fabrication techniques, thus deferring its progress.

III. RECENT PROGRESS ON PROBE MEMORIES

The aforementioned physical drawbacks severely restrict the commercialization of probe-based memory and because of this reason, probe-based memory has gradually attained less attention from global market than its competitor such as Flash memory. Nevertheless, the potential of probe-based memories to provide for higher recording density and fast write/readout speed than Flash can not be overlooked. Therefore, tremendous efforts have been devoted either to improving the physical performances of conventional probe memories through innovating probe or storage medium, or to exploring some novel probe storage means, which is presented below.

Recently a novel magnetic probe memory that combines the write mechanism of thermomechanical probe memory with a ferromagnetic shape alloy (i.e., Ni-Mn-Ga) was proposed to provide for multi-bit storage function [46]. Similar to thermomechanical probe memory, a diamond probe is usually implemented to generate nanoindentations on a thin film of Ni-Mn-Ga alloy by the induced stress. This stress-induced compressive deformation makes martensite variants with the axis of easy magnetization (the crystallographic c direction) parallel to the applied stress grow, thereby altering the total magnetization. MFM is subsequently deployed to measure the resulting stress-induced magnetization change. In spite of plastic strains that causes a permanent nanoscale shape change, the previously formed nanoindentations can be restored thermoelastically or by an externally applied magnetic field. According to these encouraging features, a series of 5×5 arrays of indentations have been fabricated on the polished $\{100\}$ face of the Ni-Mn-Ga single crystal with loading forces ranging from 5 to 26 μN. As revealed by the following MFM images, these deformed regions clearly indicate a localized change in the magnetic stray field from neutral to strong contrast, as illustrated in Figure 5(a). A more attractive

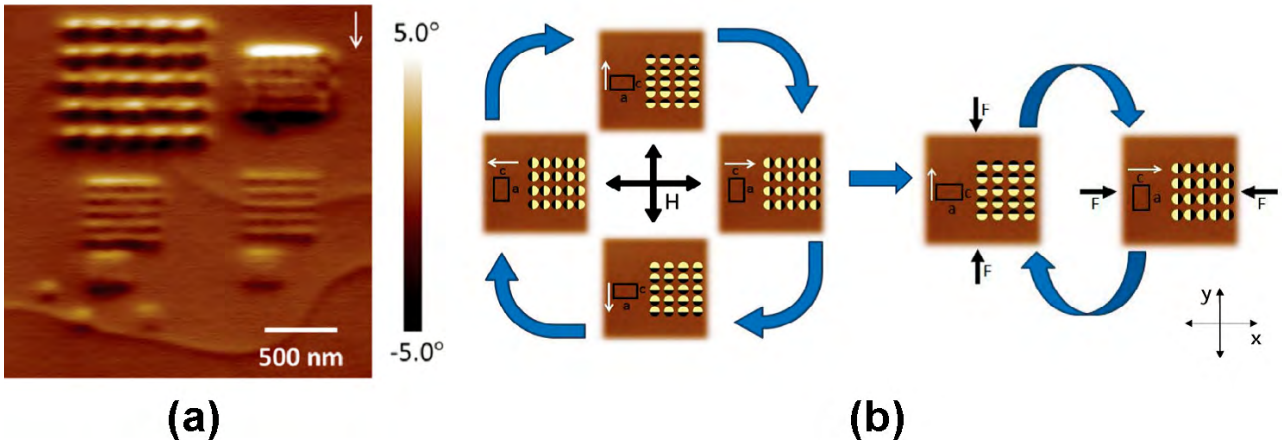

FIGURE 5. (a) MFM image of 5 × 5 indentation arrays showing the patterning of magnetic information on Ni-Mn-Ga using nanoindentation. (b)Schematic illustrating the four magnetic memory states. Reprinted with permission from [46].

fact is that the crystallographic c direction can be switched to one of two orthogonal axes x and y through twin boundary motion facilitated by an appropriate applied magnetic field or mechanical stress orthogonal to the directionality of the dark/bright contrast, while the magnetization vector for each crystallographic state controlled by twin boundary motion can be magnetically switched 180°. As a result, the possibility of achieving a four-state magnetic memory system by changing the magnetization direction through twin boundary motion, has been experimentally demonstrated (Figure 5(b)), leading to several potential applications such as quaternary non-volatile memory and Boolean operations.

In order for ferroelectric probe memory to suit practical use, its unfavorable readout operation needs to be mitigated. Piezoelectric force microscopy (PFM) readout mode is one possible method to circumvent this limit [47]. PFM readout is performed by bringing a probe tip in contact with a sample. A small alternating voltage is applied between tip and sample and the readout response consequently depends on the polarization state of the ferroelectric storage medium, which can be sensed as a readout signal by PFM at a frequency below the cantilever resonance. Another non-destructive readout approach is to take advantage of scanning nonlinear dielectric microscopy (SNOM). The SNOM readout depends on an alternating voltage applied between the SNOM probe and the ferroelectric storage medium, which induces a nonlinear dielectric response. Such a non-linearity results in a variation on the capacity of the storage medium that can subsequently alter the resonance frequency of the probe cantilever whose variation can be detected to discern the polarization state. Subnanometer and atomic scale resolutions for ferroelectric domain and surface observation of semiconductors were obtained, respectively, much higher than PFM readout. The aforementioned superiorities compared with conventional counterpart render ferroelectric probe memory based on SNOM up to 13.2 Tbits/in^2 for one-dimensional dot array and 4 Tbits/in^2 for two dimensional dot array writing, respectively [48], as illustrated in Figure 6(a), Recently, a HDD-type ferroelectric probe memory based on SNOM has been proposed to allow for a write rate of 20 Megabits per second (Mbps) and a readout rate of 2 Mbps, close to the idea write and readout rates of HDDs (∼1 Gbps) [49]. It is possible to further increase the readout rate to 10 Mbps by replacing the congruent lithium tantalite (CLT) with PZT, and the practicality of achieving 3.4 Tbits/in^2 based on HDD-type ferroelectric probe memory has also been demonstrated [49], [50].

Another promising non-destructive readout approach is to use a so-called resistive probe having an electric field sensor integrated at tip apex [51]. When this resistive probe that normally has p-type Si body and n-type Si incline is in contact with ferroelectric storage medium where a probe-medium voltage is applied, resistance of the integrated sensor shows a field-dependent property, which is thus regarded as readout signals. The spatial resolution of the resistive probe is somewhat poor (∼200 nm) even if the electric field sensor is aligned with the tip apex [52]. However, it was reported that using a wedge-shape tip can effectively reduce the spatial resolution to ∼25 nm [53], [54], corresponding to an areal density of 1 Tbit/in^2, as depicted in Figure 6(b). A HDD-type ferroelectric memory using resistive probe was also developed [51], which implemented a HDD writer and a resistive probe sensor. Such a device deploys an air-bearing slider to sustain an air gap of about 8 nm between the head and the medium, serving as tunneling barrier where the charges can flow, as in the case of alumina capped ferroelectric thin films.

According to previous findings, the write/readout performances of phase-change electrical probe memory aggressively pertain to the electrical, thermal, and geometrical properties of its capping and under layer, while previously lack of experimental measurements. In order to genuinely model the practical physical processes involved in electrical probe device, the electrical resistivities of the DLC capping and TiN under layers were measured as a function of different thicknesses. It was found that the electrical resistivity of the DLC film is almost inversely proportional to its thickness,

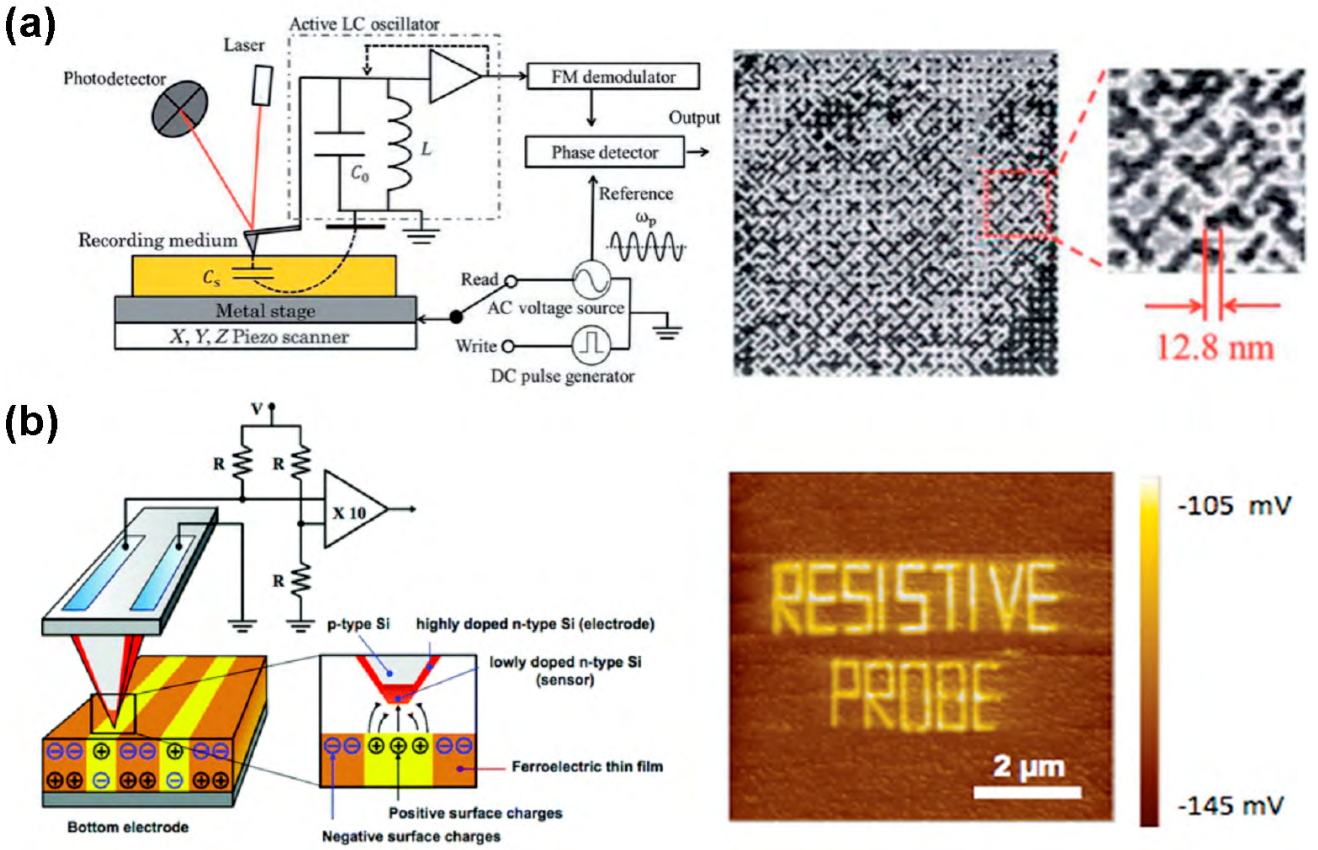

FIGURE 6. Ferroelectric probe memory operated in non-destructive mode. (a) Schematic diagram of ferroelectric probe memory based on SNOM (left) and its resulting density of 4 Tbit/in^2 with a bit spacing of 12.8 nm (right). (b) Schematic diagram of ferroelectric resistive probe memory (left) and its resulting readout image of artificially polarized domains with letters showing "RESISTIVE PROB" (right). (a) Reproduced with permission from [48]. (b) Reproduced with permission from [53].

which ranges from 0.01 to 1 Ωm with film thickness shrunk from 30 to 5 nm. Compared with DLC capping, the electrical resistivity of the TiN bottom presents a constant value of $\sim 10^{-5}$ Ωm, particularly for its thickness greater than 10 nm [55]. For this reason, the TiN bottom electrode previously optimized to have a 40 nm thickness with an electrical conductivity of 10^5 $\Omega^{-1}\mathrm{m}^{-1}$, can be achieved experimentally, while the theoretically optimized DLC capping layer with a thickness and an electrical conductivity of ∼5 nm and ∼50 $\Omega^{-1}\mathrm{m}^{-1}$, still remains challenged. In spite of this, DLC film was also reported to exhibit threshold switching characteristic due to a conjugated network of sp^2-bonded carbon cluster that forms a conductive filament connecting top electrode with bottom electrode [56]. As indicated in previous literatures, a 5 nm thick tetrahedral amorphous carbon (i.e., one typical type of DLC) film when subjected to a voltage of 3 V results in an electrical conductivity of 100 $\Omega^{-1}\mathrm{m}^{-1}$ [57]. As a result, it is reasonable to speculate that the electrical conductivity of a 2 nm thick DLC film may reach 100 $\Omega^{-1}\mathrm{m}^{-1}$ during the write process of phase-change electrical probe memory. Therefore, a pure three-dimensional (3D) electro-thermal and phase-transformation model was recently proposed to assess its write and readout function under the environment of multi-bit array [58], [59]. The investigated architecture shown in Figure 7(a) that comprises a 10 nm thick GST layer squeezed by a 2 nm thick DLC capping of an electrical conductivity and a thermal conductivity of 50 $\Omega^{-1}\mathrm{m}^{-1}$, and 0.5 $\mathrm{Wm}^{-1}\mathrm{K}^{-1}$, respectively, and a 40 nm thick TiN layer of an electrical conductivity, and a thermal conductivity of 5×10^5 $\Omega^{-1}\mathrm{m}^{-1}$, and 12 $\mathrm{Wm}^{-1}\mathrm{K}^{-1}$, respectively, not only enables an areal density of greater than 1Tbit/in^2, but also leads to the minimal thermal and readout cross-talk effects, as illustrated in Figures 7(a).

Although the capability of the aforementioned design to provide for ultra-high storage capacity while with the immunity to the write/read interferences has been demonstrated, its application prospect is severely impaired by the excessive temperature caused in DLC capping, thus failing the amorphization process. Such a high temperature is mainly induced by the much lower thermal conductivity of the DLC capping than probe and GST media [60], [61], which consequently suppresses the heat diffusion. This suggests that using a capping layer with fairly high thermal conductivity may effectively address this issue. However, increasing the thermal conductivity of the capping layer undoubtedly deteriorates the heat dissipation effect towards surrounding environment and may require larger pulse to achieve required temperature. As a result, the electrical conductivity of the capping

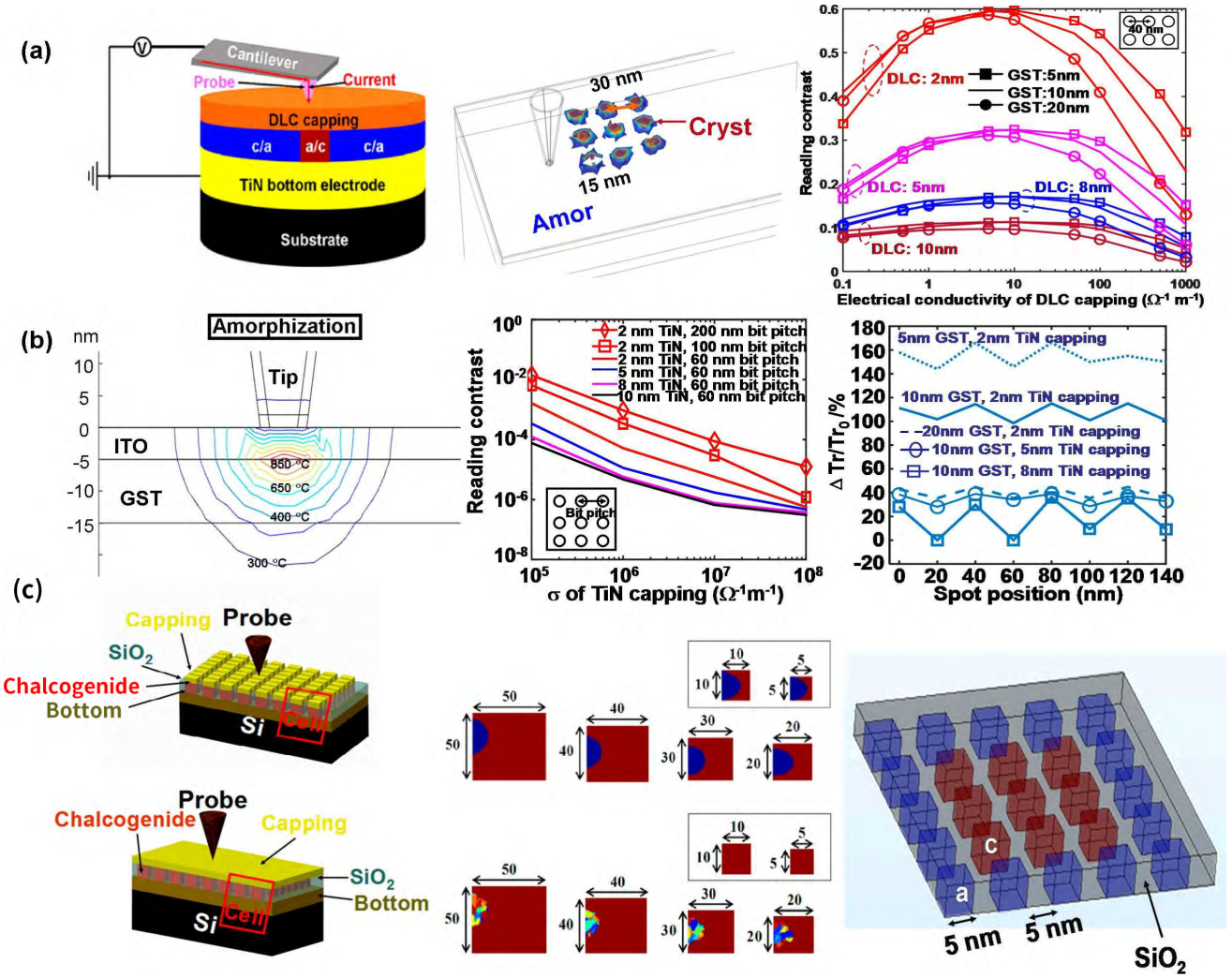

FIGURE 7. Recent advances on electrical probe phase-change memories (a) An optimized phase-change media stack based on DLC capping and TiN bottom layers (left), The resulting crystalline bit array and thermal cross-talk effects from this optimized architecture is shown in middle panel. The right panel exhibits the reading contrast as a function of the electrical and geometrical properties of the DLC capping and GST layers based on the optimized structure. (b) The temperature distribution inside an ultra electrically conductive capping layer (ITO in this case) during amorphization process. Using such a capping layer causes a very weak reading contrast, revealed in middle panel. This drawback can be alleviated by an optics means that considers device transmission as readout signals, shown in right panel. (c) Schematic of electrical probe patterned phase-change memory with patterned capping (left top) and continuous capping layers (left bottom). The obtained crystalline bit from these two designs are illustrated in middle and right panels, respectively. (a) Reproduced with permission from [58], [59]. (b) Reproduced with permission from [62], [64]. (c) Reproduced with permission from [66], [67].

layer needs to be further boomed to generate adequate joule heating for a low pulse. TiN and Indium Tin Oxide (ITO) with an electrical conductivity and a thermal conductivity of $1.25 \times 10^6\ \Omega^{-1}\mathrm{m}^{-1}$, and 4 $\mathrm{Wm}^{-1}\mathrm{K}^{-1}$, respectively, are two typical medium that satisfy above demand and the practicality of using these two medium for the capping layer of phase-change electrical probe memory has most recently been studied [62], [63], as shown in Figure 7(b). As revealed by Figure 7(b), due to their relatively high thermal conductivity, the maximal temperature inside the capping layer has been limited to 1000 °C and 850 °C for TiN and ITO capping, respectively, much lower than their melting point (i.e., ∼3200 °C for TiN and ∼1400 °C for ITO). This undoubtedly ensures the thermal stability of designed devices. Additionally, the ultra-high electrical conductivity of either TiN or ITO layer can to some extent offset the heat loss and guarantee phase-transformation occurring for a fairly low write pulse. The ability to achieve multi-Tbits/in^2 density based on these novel capping design has also been proved in Figure [62], [63]. However, the capping layer with ultra-high electrical conductivity was found to result in indistinguishable reading contrast difference between crystalline and amorphous phases [64]. This is mainly because the ultra-high electrical conductivity of the capping layer induces strong current spreading effect that drives readout current flowing along the capping layer other than focusing on the targeted bit. Such a spreading effect is more pronounced particularly for the case of reading amorphous bit from crystalline background, as majority of readout current via capping layer flow towards the crystalline background, thus making amorphous

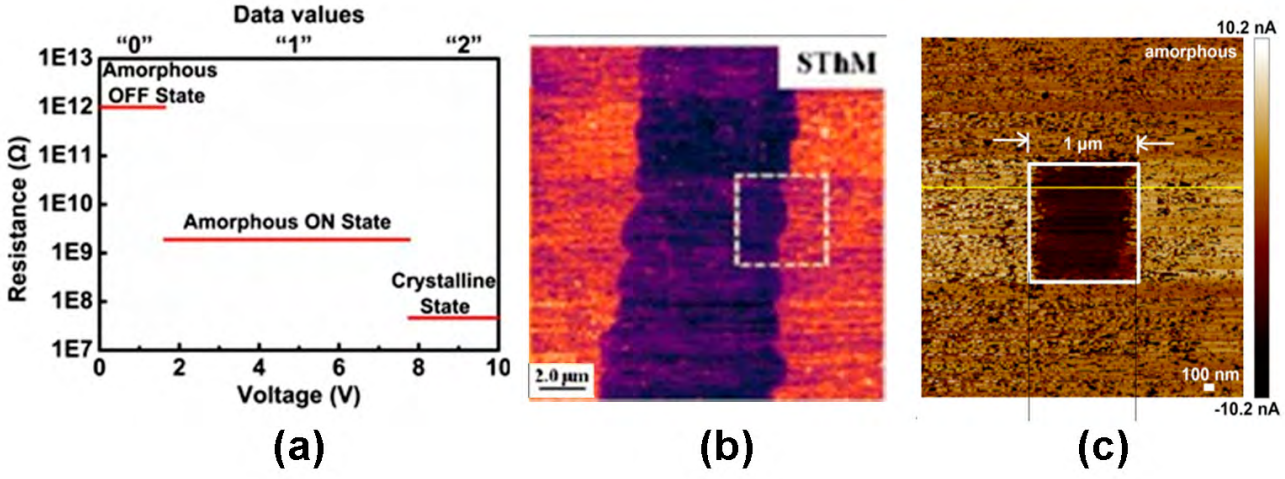

FIGURE 8. Alternative approaches for density enhancements based on electrical probe phase-change memory. (a) Three different resistance states of GST media induced by electrical probe, revealing a possibility of multi-level recording. (b) SthM image with 8 μm scan size, leading to a crystalline line written into 200 nm GeTe. (c) AFM topography image showing crystallized region of 1 μm in a 3 μm as-deposited amorphous $GeTe_6$ film. (a). Reproduced with permission from [68]. (b) Reproduced with permission from [69]. (c) Reproduced with permission from [70].

bit indistinguishable from crystalline background, as revealed in Figure 7(b). It is obviously not possible to improve the reading contrast by directly tailoring the geometrical and electrical properties of the media stack. In this case, a novel optical means to sense the written bits from un-written region has most recently been devised [64] To detect the data, a mobile laser beam, via a scanning near-field optical microscopy, is focused on the surface of the media stack. As the GST media shows distinct variation on light transmission /absorption coefficient between amorphous and crystalline phases, the resulting light transmittance when the laser beam is focused on the written bit sharply differs from that when focused on the un-transformed region, thereby accomplishing the readout process. It should be noticed that the probe-sample gap and the aperture size of the SNOM probe need to be determined carefully in order for the focused laser spot to fit the size of the written bit [65]. Results depicted in Figure clearly indicated that device transmission presents a strong variation with respect to the laser spot movement for both crystalline and amorphous cases, allowing for maximal transmission contrast of 25% and 20% for amorphous and crystalline cases, respectively, as demonstrated in Figure 7(b).

Electrical probe memory using patterned GST media [66], as illustrated in Figure 7(c), is another promising design targeted for ultra-high density, while eliminating the 'halo' that previously appears during the erasure of crystalline bits. Its geometry is very analogous to the conventional electrical probe memory except that the previous continuous GST media is replaced by numerous patterned cells isolated by insulator regions (e.g., SiO_2). Besides, to protect each cell from oxidation and wear, a capping layer is also patterned and deposited above each GST cell. As the isolated part exhibits ultra-low electrical and thermal conductivities, the unwanted current spreading phenomenon can be largely suppressed, hence minimizing the thermal and readout cross-talk effects. For this reason, the crystalline 'halo' previously present during the erasure of amorphous bit can be completely avoided using this patterned design. Triggered by its attractive features, a patterned probe memory structure that adopts 5×5 nm GST cells separated by a 3 nm wide SiO_2 spacer sandwiched between a 10 nm thick TiN capping and a 10 thick TiN bottom layers, is proposed to offer a storage density up to 10 Tbits/in^2 as well as great thermal stability [66], as demonstrated in Figure 7(c) However, such a memory design requires precise probe alignment with GST cells to avoid record/readout errors. Additionally, fabricating such a device involves the patterning of both capping and GST medium, increasing its manufacture complexity. To improve this, a novel patterned probe memory architecture that replaces patterned capping cells by a continuous capping layer was recently proposed [67], as illustrate in Figure 7(c). By appropriately choosing the geometrical and electrical properties of the capping layer, the readout current can partially flow towards the targeted bit despite the probe misalignment, which provides better fault tolerance. The possibility of writing a bit array with Tbits/in^2 density by this device was also demonstrated, as depicted in Figure 7(c).

In addition to shrinking probe size, the recording density of electrical probe phase-change memory can be also enhanced using multi-level strategy, as demonstrated in Figure 8(a). Using different voltage pulses successfully induced three distinct resistance states of GST media, which corresponds to three data values, i.e., '0', '1', and '2' to achieve multi-level operations [68]. Besides this, some other Chalcogenide alloy have been recently considered as the storage medium of electrical probe memory to replace GST media. One alternative media is GeTe (GT) alloy that shows a large thermal property difference between its crystalline and amorphous phases. Therefore, the readout process of probe memory with GT media was performed by bringing a scanning thermal

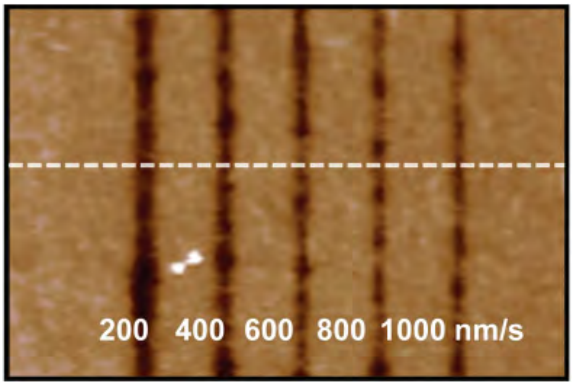

FIGURE 9. AFM topograph of patterned crystalline GeTe lines. Reproduced with permission from [71].

microscopy in proximity to the GT surface to detect its thermal property variations due to different heat flow between probe and sample, as illustrated in Figure 8(b). This opens a new way for the write and readout operation of electrical probe phase-change memory [69]. Another promising storage media is $GeTe_6$ alloy that exhibited low power threshold switching and an extremely low steady state current [70]. Its phase-transformation behavior from as-deposited amorphous to crystalline phases was also verified, as illustrated in Figure 8(c).

Exciting progress was also recently made on phase-change thermal probe memory that presents several advantages when compared with its electrical counterpart, including great robustness and immunity to bottom electrode. In order to attenuate the device complexity, a novel form of phase-change thermal probe memory taking advantage of an electrically heated tip was devised [71]. According to this design, the heated probe comprises a single crystal Si cantilever with a doped tip region where current flows through the tip induces local heating. The resulting thermal energies dissipated from such heated probe can increase the temperature inside the chalcogenide film underneath the probe and induce the highly localized phase transformation when reaching the required temperature. 1 μm crystalline square patterns, as illustrated in Figure 9, were therefore attained by varying the dissipated probe powers between 2.38 mW and 9.06 mW, while scanning tip at a speed of 500 nm/s for $\sim$20 minutes over GeTe films. This design enables a means towards flexible electronic and photonic applications, as the crystallization extent and the resultant feature width and depth can be easily altered by adjusting the tip temperature and write speed.

Aforementioned introductions are mainly concentrated on the improvements of already existing probe memory devices. Some new forms of probe memories have emerged likewise. Aggressive progress recently devoted to resistive random access memory made resistive materials another prospective storage media for electrical probe memory. Similar to chalcogenides, resistive materials usually exhibit a reversible resistive switching behaviour between LRS and HRS in a highly localized region confined by a nanoscale electrical probe, thus realizing the storage function. Pioneered by the findings of resistive switching phenomenon in single crystalline NiO hetero-structured nano-wires and in VO_2 thin films according to conductive probes[72], several prototypical devices based on various resistive materials such as TiO_2, $SrTiO_2$, and MoO_x [73]–[75], have been proposed, as illustrated in Figure 10. Their possible switching mechanism is reportedly due to formation and rupture of conductive filaments between top electrode and bottom electrode, controversially owing to an electroforming step that causes inhomogeneous oxygen vacancies [76]. However, it was most recently shown that electroforming process barely affects the resistive switching behaviour of Cu doped ZnO films and its resistive switching behaviour can only be sustained by controlling the scan rate and scan time [77]. Another experimental observation based on Time of Flight Secondary Ion Mass Spectrometry (TOF-SIMS) that ^{18}O ions mainly exist in the surface vicinity within the positively biased region of NiO films reveals that the depletion or accumulation of oxygens ions at the bottom electrode interface caused by oxygen migration within the NiO film changes the film conductivity [78]. Additionally, probe-induced resistive switching behavior has been found on organic-inorganic lead halide perovskite materials ($CH_3NH_3PbI_{3-x}Cl_x$) [79]. As illustrated in Figure 11(a), the media stack is made up of a $CH_3NH_3PbI_{3-x}Cl_x$ film deposited on FTO substrate that also serves as a bottom electrode. Different probe materials that include silver epoxy, copper and graphite were implemented to observe their impact on the resulting resistive switching. It was revealed that all three probe materials lead to a bipolar resistive switching behavior only induced by a positive voltage applied to the probe. Another intriguing finding is that such switching characteristic shows strong probe position dependence for graphite and copper probe materials, while exhibiting probe position independence for silver epoxy probe material. The switching mechanism of such a resistive material was reportedly attributed to the ion migration through the perovskite layer along the direction of applied electric field. Prior to applying stimulus, the iodide vacancies are distributed uniformly across the perovskite film, leading to a maximum gap between probe and FTO substrate. In this case, applying a positive voltage can push positive iodide vacancies toward the FTO substrate, and the subsequent accumulation of these vacancies finally forms a conductive filament to switch the device from high resistive state to low resistive state, depicted in Figure 11(a). To restore the memory, a negative voltage is applied to accumulate the negative iodide ions near the anode to fill up the vacancies, thus rupturing the conductive filament. Differing from phase change probe memory, capping layer is not employed in this resistive probe memory design. The stability of the perovskite film when subjected to oxidation and humidity therefore become highly important. To evaluate this, the resistive switching behavior of the aforementioned device was investigated as a function of its exposure time to air in terms of the resulting current-voltage (I-V) curve, resulting in Figure. No noticeable difference was

observed between the measured I-V curves before and after exposure, indicating a good stability.

Carbon-based resistive memory has recently received considerable attention because of its bond-reorganization switching process between conductive sp^2-rich state and resistive sp^3-rich state that allows for superior scaling potential, fast switching speed, and long retention time. As a result, the possibility of inducing resistive switching of carbon-based materials by conducive AFM was realized on a 20 nm amorphous carbon film deposited on 40 nm thick TiN bottom electrode [80], as schematically shown in Figure 11(b). The aforementioned PtSi probe tip was implemented to trigger the threshold switching, and to generate the conductive dots with a diameter of 20∼30 nm. The topography map and the resistance map of the region, depicted in Figure 11(b), reveal hardly any change in *sample topography, but a significant localized decrease in resistance. Such a switching behaviour was extensively attributed to the formation and rupture of low resistive sp^2 filaments inside high resistive sp^3 matrix, whereas the detailed physics behind the reported sp^2/sp^3 conversion remains unclear. One speculation ascribed the sp^2/sp^3 conversion to the thermal effect that the resulting joule heating from tunnel current yields a formation of graphitic filaments inside the insulated matrix [80]. Another plausible hypothesis interpreted sp^2/sp^3 conversion as an outcome of electric field-induced mechanism that the applied electric field intensity above the threshold value remarkably increases the reaction rate of sp^2/sp^3 conversion [81].* Most recently an innovative form of probe storage memory based on the tip-enhanced bulk photovoltaic (BPV) effect has been proposed [82]. As shown in Figure 11(c), a photo-responsive cell usually made of $BiFeO_3$(BFO) thin film is connected to an electronic memory element consisting of an AFM probe and a storage medium exhibiting an electric field-induced property such as ferroelectric materials. The photo-responsive cell under the illumination of a laser source releases the photocurrent that can flow through the electronic memory device and is consequently collected by the AFM tip. This can considerably enhance the electric field underneath the probe tip due to the BPV effect, thus to change the physical properties of the storage medium inside the electronic memory. It write and read operations are schematically described in Figure. During the write process, the electronic memory having a $PbZr_{0.2}Ti_{0.8}O_3$ (PZT) thin film is scanned under the AFM probe operated in contact mode, allowing for photocurrent flowing from BFO cell, via PZT, into the AFM tip. The polarity change of the photocurrent controlled by the illumination position to the electrode can also switch the electric field underneath the tip, thus reversing the PZT ferroelectric polarization upward and downward. It readout operation can be achieved by either piezoelectric force microscopy (PFM) that shows a clear 180° phase change or current mapping of the scanned area of the PZT that exhibits a giant resistance contrast. Such an optically controlled electronic memory reportedly leads to a very small current (∼few pA) to induce required electric field for coercivity reversal of the PZT film, and a short photoresponse time of ∼10 μs. This photo-driven AFM tip writing mechanism can be also applied to another solid-state memory platform, i.e., quasi-two dimensional electron gas (q-2DEG) at $LaAlO_3/SrTiO_3$ (LAO/STO) interface. Using the photo-induced electric field underneath the AFM tip enables a hysteretic switching behavior at the LAO/STO interface, owing to a formation of nanoscale conducting channels, as illustrated in Figure 8(b). The subsequent PFM phase image clearly shows two different patterns with clear phase contrast.

IV. CONCLUSIONS

The prosperity of information technology today produces a large volume of digital data that needs to be stored. This simultaneously requires a dramatic increase on the storage capacity of mass storage device. The mainstream storage devices today include HDDs, solid-state drive, and Flash memory. However, their respective physical limits severely handicap their suitability for next generation mass storage demand, and only half of the total digital information is estimated to be stored in HDDs and Flash in the future [51]. Under this circumstance, developing a novel form of memory device to meet future storage demand is extremely necessary.

Probe-based storage memory was one of the most promising contenders due to its attractive potential for ultra-high density and therefore received tremendous interest during last decade. Nevertheless, some formidable technology barriers gradually degraded researchers' interest in probe-based memories, and because of this, this technology is yet to be commercialized so far. In spite of this pessimistic status, its ability to potentially provide for higher memory density and lower cost per bit than HDDs and Flash can not be underestimated, and substantial efforts have recently been made to overcome aforementioned issues, majorly focused on ferroelectric probe memory and electrical probe phase-change memory. Recent advances on ferroelectric probe memory were dedicated to the improvements of its destructive readout mechanism, achieved by SNOM and field-effect transistor-type probe. Most recently HDD-type ferroelectric data storage test systems based on both SNOM and resistive probe have emerged, respectively, to produce multi $Tbit/in^2$. A more exciting fact is that several novel probe materials such as platinum iridium [40], carbon nanotube [83], and hard HfB_2 have been evaluated to mitigate tip endurance up to 8 km of sliding [84]. Due to the popularity of phase-change memory, electrical probe phase-change memory has been recently undergoing more intensive research than other probe memories. The main issue of electrical probe phase-change memory stems from its difficulty in amorphization. To circumvent this drawback, the DLC capping layer that was widely adopted in previous designs was replaced with other coating medium with ultra-high electrical conductivity and fairly high thermal conductivity such as TiN and ITO. This can effectively avoid the excessive temperature inside the capping layer while reducing the write energy consumption. However, using a capping layer with ultra-high

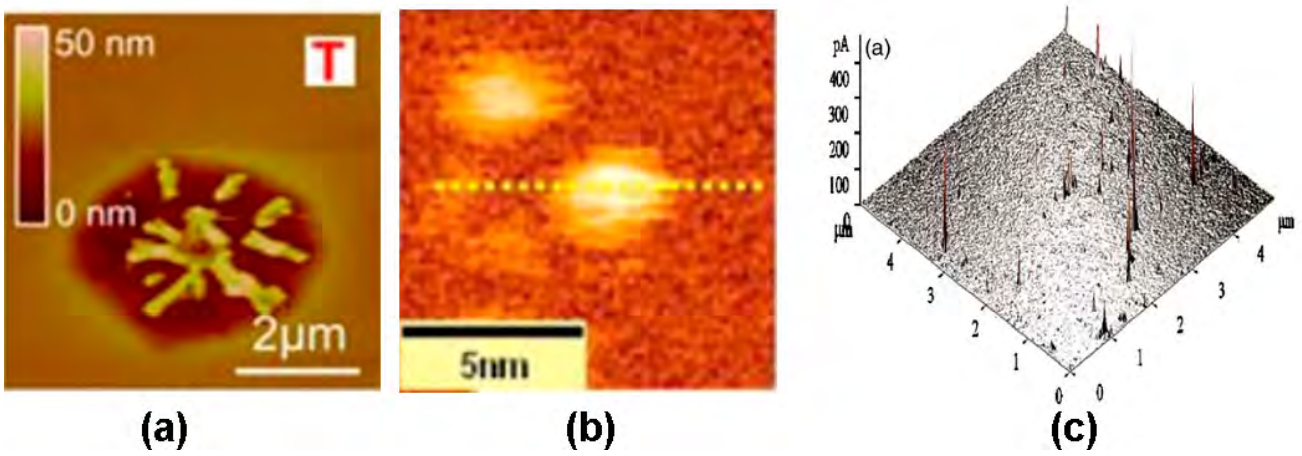

FIGURE 10. Conductivities maps of (a) TiO_2, (b) $SrTiO_2$, and (c) MoO_x films. (a). Reproduced with permission from [73]. (b) Reproduced with permission from [74]. (c) Reproduced with permission from [75].

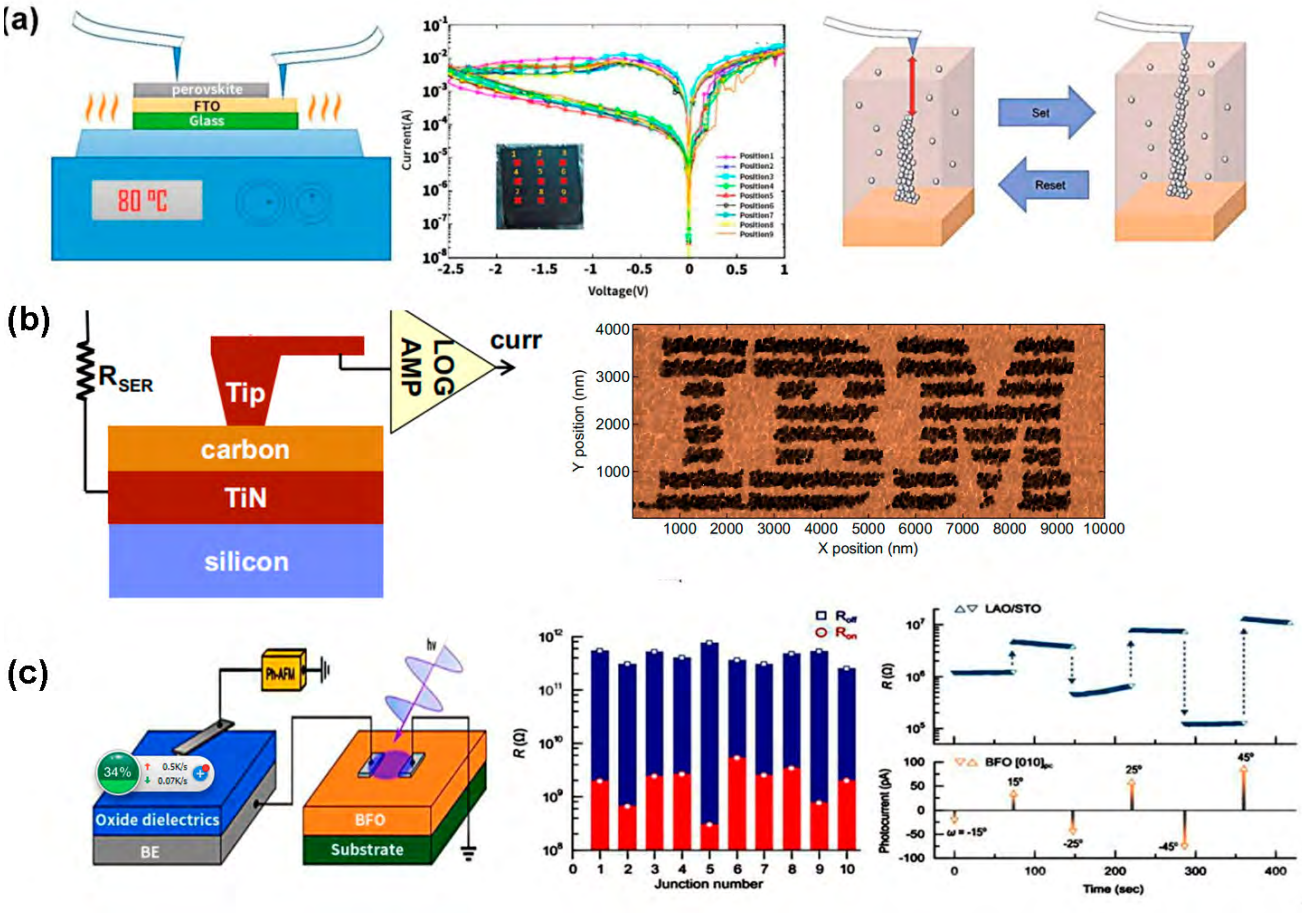

FIGURE 11. Recent advances on some innovative forms of probe-based memories. (a) Experimental setup of electrical probe resistive memory based on perovskite film (left). Its I-V curves fro different probe positions and the likely switching mechanism are described in middle and right panels, respectively. (b) Schematic of carbon-based probe memory (left) and its resistance patterning (right). (c) Schematic of photo-induce probe memory (left). The resulting resistance state in FTJ and Lao interface are also revealed in middle and right panels, respectively. (a). Reproduced with permission from [79]. (b) Reproduced with permission from [80]. (c) Reproduced with permission from [82].

electrical conductivity consequently causes a strong readout cross-talk effect that generates undiscernible readout signals between crystalline and amorphous bits. This can be alleviated by detecting device transmission variations base on SNOM techniques. Another improved version of electrical probe patterned phase-change memory that patterns storage medium into numerous cells separated by insulated region, which can encouragingly overcome the resulting

TABLE 1. Performances comparison of different forms of probe memories.

	Thermomech	Magnetic	Ferroelectric	Phase-change	Thermal	Resistive	Desired
Density	4 T/in^2	60 G/in^2	4 T/in^2	3.3 T/in^2	3.3 T/in^2	1 T/in^2	>1 T/in^2
Read Speed	40 kb/s	10 b/s	2 Mb/s	50 Mb/s	N/A	200 Mb/s	>10 Mb/s
Write Speed	1 Mb/s	10 b/s	50 kb/s	50 Mb/s	100 Mb/s	200 Mb/s	>10 Mb/s
Retention	N/A	20 years	10 years	50 years	50 years	50 years	>50 years
Endurance	N/A	3×10^{16}	10^{14}	10^{9}	10^{4}	10^{10}	$>10^{10}$
Multi-level	No	Yes	No	Yes	No	Yes	Yes

cross-talk effects. Moreover, excited by developments of lithography techniques, the cell size can be further shrunk to increase the recording density. In addition to the advances on conventional probe memories, some innovative probe memory including electrical probe resistive probe memory carbon-based probe memory, and photo-induced probe memory, thus paving a new route for probe memory towards its future applications. The characteristic comparison for different probe memories is shown in Table 1.

Despite recent resuscitation, probe-based memories are still facing many issues in order to challenge HDDs and Flash memory. Although a non-destructive readout mechanism for ferroelectric probe memory has been proposed, its recording density however does not seem to be advantageous compared with HDDs and Flash, likely caused by tip wear. Electrical probe phase-change probe memory is able to induce an areal density greater than 10 Tbits/inch^2, whereas the difficulty in experimentally its amorphization is witnessed. Although this issue can be addressed using optical means, this undoubtedly makes write/read system much more complex than the original design, and may not be suitable for practical application. Photo-induced probe memory allows for small energy consumption and fast write speed. Nevertheless, it requires an integration of photo-induced element with an electronic memory element, severely harming the resulting integration density. Besides, the size of probe tip used for photo-induced probe memory is relatively large ($\sim\mu$m), thereby resulting in much lower storage density than its compatriots. In this case, its storage capability with nanosca sized probe remain questionable. According to above comparisons, electrical probe resistive probe memory seems to be the most promising candidates to prevail HDDs and Flash for next-generation mass storage device. As the resistive switching behavior is mainly governed by electrical stimulus, the encapsulation probe tip with super-conductive region at tip apex that was originally designed for electrical probe phase-change memory is also perfectly suitable for electrical probe resistive memory to mitigate tip wear. Moreover, the advantageous traits of resistive random access memory such as ultra-high density, fast write speed, and low energy consumption can be inherited by electrical probe resistive memory. Most importantly, due to its super stability to oxygen and air, such a device can be fabricated without demanding for a coating layer, rendering it highly suitable for practical use.

REFERENCES

[1] D. Reinsel, J. Gantz, and J. Rydning, "Data age 2025: The evolution of data to life-critical, IDC White Paper," Int. Data Corp., Framingham, MA, USA, White Paper 1, 2017, pp. 1–25.

[2] M. D.'Aquino, V. Scalera, and C. Serpico, "Analysis of switching times statistical distributions for perpendicular magnetic memories," *J. Magn. Magn. Mater.*, vol. 475, pp. 652–661, Apr. 2019.

[3] A. V. Kimel and M. Li, "Writing magnetic memory with ultrashort light pulses," *Nature Rev. Mater.*, vol. 4, pp. 189–200, Feb. 2019.

[4] F. Shiono, H. Abe, T. Nagase, T. Kobayashi, and H. Naito, "Optical memory characteristics of solution-processed organic transistors with self-organized organic floating gates for printable multi-level storage devices," *Org. Electron.*, vol. 67, pp. 109–115, Apr. 2019.

[5] M. Gu, Q. Zhang, and S. Lamon, "Nanomaterials for optical data storage," *Nature Rev. Mater.*, vol. 1, no. 12, Dec. 2016, Art. no. 16070.

[6] B. Bharat, "Historical evolution of magnetic data storage devices and related conferences," *Microsyst. Technol.*, vol. 24, no. 11, pp. 4423–4436, Nov. 2018.

[7] S. Furrer, M. A. Lantz, P. Reininger, A. Pantazi, H. E. Rothuizen, R. D. Cideciyan, G. Cherubini, W. Haeberle, E. Eleftheriou, J. Tachibana, N. Sekiguchi, T. Aizawa, T. Endo, T. Ozaki, T. Sai, R. Hiratsuka, S. Mitamura, and A. Yamaguchi, "201 Gb/in^2 recording areal density on sputtered magnetic tape," *IEEE Trans. Magn.*, vol. 54, no. 2, Feb. 2018, Art. no. 3100308.

[8] G. Binnig, C. F. Quate, and C. Gerber, "Atomic force microscope," *Phys. Rev. Lett.*, vol. 56, no. 9, pp. 930–933, Mar. 1986.

[9] P. Vettiger, M. Despont, U. Drechsler, U. Durig, W. Haberle, M. I. Lutwyche, H. E. Rothuizen, R. Stutz, R. Widmer, and G. K. Binnig, "The 'Millipede'—More than thousand tips for future AFM storage," *IBM J. Res. Develop.*, vol. 44, no. 3, pp. 323–340, May 2000.

[10] H. Pozidis, W. Haberle, D. Wiesmann, U. Drechsler, M. Despont, T. R. Albrecht, and E. Eleftheriou, "Demonstration of thermomechanical recording at 641 Gbit/in$_2$," *IEEE Trans. Magn.*, vol. 40, no. 4, pp. 2531–2536, Jul. 2004.

[11] B. Gotsmann, A. W. Knoll, R. Pratt, J. Frommer, J. L. Hedrick, and U. Duerig, "Designing polymers to enable nanoscale thermomechanical data storage," *Adv. Funct. Mater.*, vol. 20, no. 8, pp. 1276–1284, Apr. 2010.

[12] D. Wiesmann, C. Rawlings, R. Vecchione, F. Porro, B. Gotsmann, A. Knoll, D. Pires, and U. Duerig, "Multi Tbit/in^2 storage densities with thermomechanical probes," *Nano Lett.*, vol. 9, no. 9, pp. 3171–3176, Aug. 2009.

[13] R. J. Cannara, B. Gotsmann, A. Knoll, and U. Dürig, "Thermo-mechanical probe storage at Mbps single-probe data rates and Tbit/in^2 densities," *Nanotechnology*, vol. 19, no. 39, Aug. 2008, Art. no. 395305.

[14] L. Wang, C. H. Yang, J. Wen, S. D. Gong, and Y. X. Peng, "Overview of probe-based storage technologies," *Nanosc. Res. Lett.*, vol. 11, pp. 342–355, Jul. 2016.
[15] L. Zhang, J. A. Bain, J.-G. Zhu, L. Abelmann, and T. Onoue, "The role of MFM signal in mark size measurement in probe-based magnetic recording on CoNi/Pt multilayers," *Phys. B, Condens. Matter*, vol. 387, nos. 1–2, pp. 328–332, Jan. 2007.
[16] Z. Zhong, L. Zhang, and H. Zhang, "Dependence of mark size on STM pulse voltage in heat-assisted magnetic probe recording on a cobalt–nickel–platinum thin film," *Current Appl. Phys.*, vol. 8, no. 1, pp. 57–60, Jan. 2008.
[17] L. Zhang, J. A. Bain, J.-G. Zhu, L. Abelmann, and T. Onoue, "Characterization of heat-assisted magnetic probe recording on CoNi/Pt multilayers," *J. Magn. Magn. Mater.*, vol. 305, no. 1, pp. 16–23, Oct. 2006.
[18] L. Zhang, J. A. Bain, and J.-G. Zhu, "Dependence of thermomagnetic mark size on applied STM voltage in Co-Pt multilayers," *IEEE Trans. Magn.*, vol. 38, no. 5, pp. 1895–1897, Sep. 2002.
[19] L. Zhang, J. A. Bain, J.-G. Zhu, L. Abelmann, and T. Onoue, "A model for mark size dependence on field emission voltage in heat-assisted magnetic probe recording on CoNi/Pt multilayers," *IEEE Trans. Magn.*, vol. 40, no. 4, pp. 2549–2551, Jul. 2004.
[20] T. Onoue, M. H. Siekman, L. Abelmann, and J. C. Lodder, "Probe recording on CoNi/Pt multilayered thin films by using an MFM tip," *J. Magn. Magn. Mater.*, vols. 272–276, pp. 2317–2318, May 2004.
[21] Y. Zhao, E. Johns, and M. Forrester, "A MEMS read-write head for ferroelectric probe storage," in *Proc. IEEE 21st Int. Conf. Micro Electro Mech. Syst.*, Jan. 2008, pp. 152–155.
[22] Y. Cho, S. Hashimoto, N. Odagawa, K. Tanaka, and Y. Hiranaga, "Nanodomain manipulation for ultrahigh density ferroelectric data storage," *Nanotechnology*, vol. 17, no. 7, p. S137, Mar. 2006.
[23] H. Takahashi, Y. Mimura, S. Mori, M. Ishimori, A. Onoe, T. Ono, and M. Esashi, "The fabrication of metallic tips with a silicon cantilever for probe-based ferroelectric data storage and their durability experiments," *Nanotechnology*, vol. 20, no. 36, Aug. 2009, Art. no. 365201.
[24] Y. Cho, K. Fujimoto, Y. Hiranaga, and Y. Wagatsuma, "Tbit/inch^2 ferroelectric data storage based on scanning nonlinear dielectric microscopy," *Appl. Phys. Lett.*, vol. 81, pp. 4401–4403, Dec. 2002.
[25] Y. Cho, Y. Hiranaga, K. Fujimoto, Y. Wagatsuma, and A. Onoe, "Fundamental study on ferroelectric data storage with the density above 1 Tbit/inch^2 using congruent lithium tantalate," *Integr. Ferroelectr.*, vol. 61, no. 1, pp. 77–81, Aug. 2004.
[26] Y. Cho, Y. Hiranaga, K. Fujimoto, Y. Wagatsuma, K. Terabe, K. Kitamura, and A. Onoe, "Tbit/Inch 2 data storage using scanning nonlinear dielectric microscopy," *Ferroelectrics*, vol. 292, no. 1, pp. 51–58, Jan. 2003.
[27] S. Gidon, O. Lemonnier, B. Rolland, O. Bichet, and C. Dressler, "Electrical probe storage using joule heating in phase change media," *Appl. Phys. Lett.*, vol. 85, pp. 6392–6394, Oct. 2004.
[28] C. D. Wright, M. Armand, and M. M. Aziz, "Terabit-per-square-inch data storage using phase-change media and scanning electrical nanoprobes," *IEEE Trans. Nanotechnol.*, vol. 5, no. 1, pp. 50–61, Jan. 2006.
[29] H. Satoh, K. Sugawara, and K. Tanaka, "Nanoscale phase changes in crystalline $Ge_2Sb_2Te_5$ films using scanning probe microscopes," *J. Appl. Phys.*, vol. 99, no. 2, Jan. 2006, Art. no. 024306.
[30] H. Bhaskaran, A. Sebastian, A. Pauza, H. Pozidis, and M. Despont, "Nanoscale phase transformation in $Ge_2Sb_2Te_5$ using encapsulated scanning probes and retraction force microscopy," *Rev. Sci. Instrum.*, vol. 80, no. 8, Aug. 2009, Art. no. 083701.
[31] C. D. Wright, L. Wang, P. Shah, M. M. Aziz, E. Varesi, R. Bez, M. Moroni, and F. Cazzaniga, "The design of rewritable ultrahigh density scanning-probe phase-change memories," *IEEE Trans. Nanotechnol.*, vol. 10, no. 4, pp. 900–912, Jul. 2011.
[32] X. Sun, U. Roß, J. W. Gerlach, A. Lotnyk, and B. Rauschenbach, "Nanoscale bipolar electrical switching of $Ge_2Sb_2Te_5$ phase-change material thin films," *Adv. Electron. Mater.*, vol. 3, no. 12, Dec. 2017, Art. no. 1700283.
[33] L. Wang, J. Wen, C. Yang, S. Gai, and X. S. Miao, "Optimisation of write performance of phase-change probe memory for future storage applications," *Nanosci. Nanotechnol. Lett.*, vol. 7, no. 11, pp. 870–878, Nov. 2015.
[34] L. Wang, J. Wen, C. Yang, S. Gai, and Y. Peng, "The route for ultra-high recording density using probe-based data storage device," *Nano*, vol. 10, no. 8, Sep. 2015, Art. no. 1550118.
[35] H. F. Hamann, M. O.'Boyle, Y. C. Martin, M. Rooks, and H. K. Wickramasinghe, "Ultra-high-density phase-change storage and memory," *Nature Mater.*, vol. 5, no. 5, pp. 383–387, May 2006.
[36] G. A. Shaw, J. S. Trethewey, A. D. Johnson, W. J. Drugan, and W. C. Crone, "Thermomechanical high-density data storage in a metallic material via the shape-memory effect," *Adv. Mater.*, vol. 17, no. 9, pp. 1123–1127, May 2005.
[37] V. L. Mironov and O. L. Ermolaeva, "Optimization of a data storage system based on the array of ferromagnetic particles and magnetic force microscope," *J. Surf. Invest.*, vol. 3, pp. 840–848, Oct. 2009.
[38] R. T. El-Sayed and L. R. Carley, "Analytical and micromagnetic-based modeling of quantization noise in MFM-based pulse-width-Modulation perpendicular recording," *IEEE Trans. Magn.*, vol. 40, no. 4, pp. 2326–2328, Jul. 2004.
[39] D. Gregušová, J. Martaus, J. Fedor, R. Kúdela, I. Kostič, and V. Cambel, "On-tip sub-micrometer hall probes for magnetic microscopy prepared by AFM lithography," *Ultramicroscopy*, vol. 109, no. 8, pp. 1080–1084, Jul. 2009.
[40] N. Tayebi, Y. Zhang, R. J. Chen, Q. Tran, R. Chen, Y. Nishi, Q. Ma, and V. Rao, "An ultraclean tip-wear reduction scheme for ultrahigh density scanning probe-based data storage," *ACS Nano*, vol. 4, no. 10, pp. 5713–5720, Oct. 2010.
[41] Y. Hiranaga, T. Uda, Y. Kurihashi, K. Tanaka, and Y. Cho, "Novel HDD-type SNDM ferroelectric data storage system aimed at high-speed data transfer with single probe operation," *IEEE Trans. Ultrason., Ferroelectr., Freq. Control*, vol. 54, no. 12, pp. 2523–2528, Dec. 2007.
[42] S. Raoux, F. Xiong, M. Wuttig, and E. Pop, "Phase change materials and phase change memory," *MRS Bull.*, vol. 39, no. 8, pp. 703–710, Aug. 2014.
[43] J. Tominaga and L. Bolotov, "Re-amorphization of GeSbTe alloys not through a melt-quenching process," *Appl. Phys. Express*, vol. 12, no. 1, Nov. 2018, Art. no. 015504.
[44] H. Bhaskaran, A. Sebastian, and M. Despont, "Nanoscale PtSi tips for conducting probe technologies," *IEEE Trans. Nanotechnol.*, vol. 8, no. 1, pp. 128–131, Jan. 2009.
[45] H. Bhaskaran, A. Sebastian, U. Drechsler, and M. Despont, "Encapsulated tips for reliable nanoscale conduction in scanning probe technologies," *Nanotechnology*, vol. 20, no. 10, Feb. 2009, Art. no. 105701.
[46] C. S. Watson, C. Hollar, K. Anderson, W. B. Knowlton, and P. Müllner, "Magnetomechanical four-state memory," *Adv. Funct. Maters.*, vol. 23, no. 32, pp. 3995–4001, Aug. 2013.
[47] S. V. Kalinin, S. Jesse, B. J. Rodriguez, J. Shin, A. P. Baddorf, H. N. Lee, A. Borisevich, and S. J. Pennycook, "Spatial resolution, information limit, and contrast transfer in piezoresponse force microscopy," *Nanotechnology*, vol. 17, no. 14, pp. 3400–3411, Jul. 2006.
[48] K. Tanaka and Y. Cho, "Actual information storage with a recording density of 4 Tbit/in.^{2} in a ferroelectric recording medium," *Appl. Phys. Lett.*, vol. 97, no. 9, Aug. 2010, Art. no. 092901.
[49] T. Aoki, Y. Hiranaga, and Y. Cho, "High-density ferroelectric recording using a hard disk drive-type data storage system," *J. Appl. Phys.*, vol. 119, no. 18, May 2016, Art. no. 184101.
[50] S. Hong, S. M. Nakhmanson, and D. D. Fong, "Screening mechanisms at polar oxide heterointerfaces," *Rep. Prog. Phys.*, vol. 79, no. 7, Jun. 2016, Art. no. 076501.
[51] Y. Cho and S. Hong, "Scanning probe-type data storage beyond hard disk drive and flash memory," *MRS Bull.*, vol. 43, no. 5, pp. 365–369, May 2018.
[52] H. Park, J. Jung, D.-K. Min, S. Kim, S. Hong, and H. Shin, "Scanning resistive probe microscopy: Imaging ferroelectric domains," *Appl. Phys. Lett.*, vol. 84, no. 10, pp. 1734–1736, Mar. 2004.
[53] H. Ko, K. Ryu, H. Park, C. Park, D. Jeon, Y. K. Kim, J. Jung, D.-K. Min, Y. Kim, H. N. Lee, Y. Park, H. Shin, and S. Hong, "High-resolution field effect sensing of ferroelectric charges," *Nano. Lett.*, vol. 11, no. 4, pp. 1428–1433, Mar. 2011.
[54] S. Hong, S. Tong, W. I. Park, Y. Hiranaga, Y. Cho, and A. Roelofs, "Charge gradient microscopy," *Proc. Nat. Acad. Sci. USA*, vol. 111, no. 18, pp. 6566–6569, May 2014.
[55] L. Wang, S. Gong, C. Yang, and J. Wen, "Towards low energy consumption data storage era using phase-change probe memory with TiN bottom electrode," *Nanotechnol. Rev.*, vol. 5, no. 5, pp. 455–460, Oct. 2016.
[56] F. Hui, E. Grustan-Gutierrez, S. Long, Q. Liu, A. K. Ott, A. C. Ferrari, and M. Lanza, "Graphene and related materials for resistive random access memories," *Adv. Electron. Mater.*, vol. 3, no. 8, Aug. 2017, Art. no. 1600195.
[57] T. A. Bachmann, A. M. Alexeev, W. W. Koelmans, F. Zipoli, A. K. Ott, C. Dou, A. C. Ferrari, V. K. Nagareddy, M. F. Craciun, V. P. Jonnalagadda, A. Curioni, A. Sebastian, E. Eleftheriou, and C. D. Wright, "Temperature evolution in nanoscale carbon-based memory devices due to local joule heating," *IEEE Trans. Nanotechnol.*, vol. 16, no. 5, pp. 806–811, Sep. 2017.

[58] L. Wang, J. Wen, and B. Xiong, "Nanoscale thermal cross-talk effect on phase-change probe memory," *Nanotechnology*, vol. 29, no. 37, Jul. 2018, Art. no. 375201.
[59] L. Wang, C.-H. Yang, J. Wen, and B.-S. Xiong, "Reading contrast of phase-change electrical probe memory in multiple bit array," *IEEE Trans. Nanotechnol.*, vol. 18, pp. 260–269, Mar. 2019.
[60] K. Ren, M. Zhu, W. Song, S. Lv, M. Xia, Y. Wang, Y. Lu, Z. Jib, and Z. Song, "Electrical switching properties and structural characteristics of GeSe–GeTe films," *Nanoscale*, vol. 11, no. 4, pp. 1595–1603, 2019.
[61] X.-X. Zhang, L.-Q. Ai, M. Chen, and D.-X. Xiong, "Thermal conductive performance of deposited amorphous carbon materials by molecular dynamics simulation," *Mol. Phys.*, vol. 115, no. 7, pp. 831–838, Feb. 2017.
[62] L. Wang, J. Wen, C. Yang, and B. Xiong, "Potential of ITO thin film for electrical probe memory applications," *Sci. Technol. Adv. Mater.*, vol. 19, no. 1, pp. 791–801, Oct. 2018.
[63] L. Wang, J. Wen, C. Yang, and B. Xiong, "Design of electrical probe memory with TiN capping layer," *J. Mater. Sci.*, vol. 53, pp. 15549–15558, Nov. 2018.
[64] L. Wang, C.-H. Yang, J. Wen, and B.-S. Xiong, "Electro-optical operation of electrical probe phase-change memory with ultra-high electrically conductive capping layer," *IEEE Access*, vol. 7, pp. 32327–32332, 2019.
[65] P. Bazylewski, S. Ezugwu, and G. Fanchini, "A review of three-dimensional scanning near-field optical microscopy (3D-SNOM) and its applications in nanoscale light management," *Appl. Sci.*, vol. 7, no. 10, pp. 973–983, 2017.
[66] H. Hayat, K. Kohary, and C. D. Wright, "Ultrahigh storage densities via the scaling of patterned probe phase-change memories," *IEEE Trans. Nanotechnol.*, vol. 16, no. 5, pp. 767–772, Sep. 2017.
[67] L. Wang, Z.-G. Liu, C.-H. Yang, J. Wen, and B.-S. Xiong, "Design of ultra-high storage density probe memory with patterned $Ge_2Sb_2Te_5$ layer and continuous capping layer," *Appl. Phys. Express*, vol. 12, no. 5, Apr. 2019, Art. no. 055002.
[68] F. Yang, L. Xu, J. Chen, J. Xu, Y. Yu, Z. Ma, and K. Chen, "Nanoscale multilevel switching in $Ge_2Sb_2Te_5$ thin film with conductive atomic force microscopy," *Nanotechnology*, vol. 27, no. 3, Dec. 2015, Art. no. 035706.
[69] J. L. Bosse, M. Timofeeva, P. D. Tovee, B. J. Robinson, B. D. Huey, and O. V. Kolosov, "Nanothermal characterization of amorphous and crystalline phases in chalcogenide thin films with scanning thermal microscopy," *J. Appl. Phys.*, vol. 116, no. 13, Oct. 2014, Art. no. 134904.
[70] A. Manivannan, S. K. Myana, K. Miriyala, S. Sahu, and R. Ramadurai, "Low power ovonic threshold switching characteristics of thin $GeTe_6$ films using conductive atomic force microscopy," *Appl. Phys. Lett.*, vol. 105, no. 24, Dec. 2014, Art. no. 243501.
[71] A. Podpirka, W.-K. Lee, J. I. Ziegler, T. H. Brintlinger, J. R. Felts, B. S. Simpkins, N. D. Bassim, A. R. Laracuente, P. E. Sheehana, and L. B. Ruppalt, "Nanopatterning of GeTe phase change films via heated-probe lithography," *Nanoscale*, vol. 9, no. 25, pp. 8815–8824, Jun. 2017.
[72] J. Kim, C. Ko, A. Frenzel, S. Ramanathan, and J. E. Hoffman, "Nanoscale imaging and control of resistance switching in VO_2 at room temperature," *Appl. Phys. Lett.*, vol. 96, no. 21, May 2010, Art. no. 213106.
[73] R. Münstermann, J. J. Yang, J. P. Strachan, G. Medeiros-Ribeiro, R. Dittmann, and R. Waser, "Morphological and electrical changes in TiO_2 memristive devices induced by electroforming and switching," *Phys. Status. Solidi Rapid Res. Lett.*, vol. 4, nos. 1–2, pp. 16–18, Feb. 2010.
[74] K. Szot, R. Dittmann, W. Speier, and R. Waser, "Nanoscale resistive switching in $SrTiO_3$ thin films," *Phys. Status. Solidi Rapid Res. Lett.*, vol. 1, no. 2, pp. R86–R88, Mar. 2007.
[75] D. Lee, D.-J. Seong, I. Jo, F. Xiang, R. Dong, S. Oh, and H. Hwang "Resistance switching of copper doped MoO_x films for nonvolatile memory applications," *Appl. Phys. Lett.*, vol. 90, no. 12, Mar. 2007, Art. no. 122104.
[76] M. H. Lee and C. S. Hwang, "Resistive switching memory: Observations with scanning probe microscopy," *Nanoscale*, vol. 3, no. 2, pp. 490–502, 2011.
[77] J. Xiao, T. S. Herng, J. Ding, and K. Zeng, "Resistive switching behavior in copper doped zinc oxide (ZnO:Cu) thin films studied by using scanning probe microscopy techniques," *J. Alloys Compounds*, vol. 709, pp. 535–541, Jun. 2017.
[78] C. Yoshida, K. Kinoshita, T. Yamasaki, and Y. Sugiyama, "Direct observation of oxygen movement during resistance switching in NiO/Pt film," *Appl. Phys. Lett.*, vol. 93, no. 4, Jul. 2008, Art. no. 042106.
[79] A. Shaban, M. Joodaki, S. Mehregan, and I. W. Rangelow, "Probe-induced resistive switching memory based on organic-inorganic lead halide perovskite materials," *Organic Electron.*, vol. 69, pp. 106–113, Jun. 2019.
[80] A. Sebastian, A. Pauza, C. Rossel, R. M. Shelby, A. F. Rodríguez, H. Pozidis, and E. Eleftheriou, "Resistance switching at the nanometre scale in amorphous carbon," *New J. Phys.*, vol. 13, no. 1, Jan. 2011, Art. no. 013020.
[81] Y.-J. Chen, H.-L. Chen, T.-F. Young, T.-C. Chang, T.-M. Tsai, K.-C. Chang, R. Zhang, K.-H. Chen, J.-C. Lou, T.-J. Chu, J.-H. Chen, D.-H. Bao, and S. M. Sze, "Hydrogen induced redox mechanism in amorphous carbon resistive random access memory," *Nanosc. Res. Lett.*, vol. 9, no. 1, pp. 52–56, Dec. 2014.
[82] Z.-D. Luo, D.-S. Park, M.-M. Yang, and M. Alexe, "Light-controlled nanoscopic writing of electronic memories using the tip-enhanced bulk photovoltaic effect," *ACS. Appl. Mater. Interfaces*, vol. 11, no. 8, pp. 8276–8283, Feb. 2019.
[83] N. Tayebi, Y. Narui, R. J. Chen, C. P. Collier, K. P. Giapis, and Y. Zhang, "Nanopencil as a wear-tolerant probe for ultrahigh density data storage," *Appl. Phys. Lett.*, vol. 93, no. 10, Sep. 2008, Art. no. 103112.
[84] N. Tayebi, A. Yanguas-Gil, N. Kumar, Y. Zhang, J. R. Abelson, Y. Nishi, Q. Ma, and V. R. Rao, "Hard HfB_2 tip-coatings for ultrahigh density probe-based storage," *Appl. Phys. Lett.*, vol. 101, no. 9, Aug. 2012, Art. no. 091909.

ZHI-GAO LIU received the B.S. degree in electrical engineering from Wuyi University, in 2015. He is currently pursuing the M.Sc. degree in control engineering with Nanchang Hangkong University. His research interest includes the development of novel probe-based memories.

LEI WANG received the B.Eng. degree in electrical engineering from the Beijing University of Science and Technology, Beijing, China, in 2003, the M.Sc. degree in electronic instrumentation systems from The University of Manchester, Manchester, U.K., in 2004, and the Ph.D. degree in Tbit/sq.in. scanning probe phase-change memory from the University of Exeter, Exeter, U.K., in 2009, where he was a Postdoctoral Research Fellow, from 2008 to 2011, to work on a fellowship funded by European Commission. These works included the study of phase-change probe memory and phase-change memristor. Since 2012, he has been with Nanchang Hangkong University, Nanchang, China, as an Associate Professor, where he is engaged in the phase-change memories, phase-change neural networks, and other phase-change-based optoelectronic devices and their potential applications.